42. HYDRAULIC CONDUCTIVITY OF DIATOMACEOUS SEDIMENT FROM THE PERU CONTINENTAL MARGIN OBTAINED DURING ODP LEG 112[1,2]

Janice C. Marsters[3] and Harold A. Christian[4]

ABSTRACT

This study examines the hydraulic conductivity characteristics of diatomaceous sediments from Ocean Drilling Program Sites 679 and 681 on the Peru continental margin. Constant-head tests were performed on samples from two sites. Values of hydraulic conductivity of 10^{-9} to 10^{-6} cm/s were measured at void ratios of 5.4 to 1.3. These values are lower than those typical for a silt, as the sediment is defined by grain size analyses. Diagenetic bonding of the diatomaceous fabric may significantly decrease the number of well-connected pore spaces, thus altering the tortuosity of this size fraction so that the length of the drainage path is increased.

INTRODUCTION

The *JOIDES Resolution* drilled at 10 sites on the Peru continental margin during Ocean Drilling Program (ODP) Leg 112 (Fig. 1). At all sites drilled on the shelf and upper slope of the margin, a highly concentrated subsurface brine was indicated by increasing chloride gradients in the pore fluids (Suess, von Huene, et al., 1988a). Evidence of low-chloride fluids has been found in the sediment of the midslope basins along zones of apparently increased fluid movement characterized by faults, unconformities, and coarser sediments.

The processes by which a contaminant is transported by fluid flow through the voids of a porous medium can be very complex (Rumer, 1972). Sediment accumulation results in pore fluid pressure gradients. High biogenic production leading to increased sedimentation rates is expected to cause high pore fluid pressure gradients in the Peru margin sediments. This relationship is exhibited by the frequent occurrence of fluid escape structures observed in the cores (Suess, von Huene, et al., 1988b; Lindsley-Griffin et al., this volume). These pressure gradients induce convective flow.

Thermal and chemical potential gradients can also occur. In the shallow sediments studied here, thermal gradients are not likely to be important. However, large chemical gradients have been observed to occur in the Peru margin sediment (Suess, von Huene, et al., 1988a). Gradients of chemical potential of the diffusing species are the driving force for molecular diffusion. The processes of molecular diffusion include diffusion of the contaminating substance across streamlines and adsorption of the contaminating substance onto solid boundaries of the pore system.

Shallow diagenesis occurs in the sediment of the Peru margin (Suess, von Huene, et al., 1988b). Diagenetic redistribution involves dissolution of a given substance, its migration, and its reprecipitation within the same sediment or rock unit (Berner, 1980). Two basic transport phenomena are likely involved in the migration of solutes and diagenesis in the sediment of the Peru margin. The first, convection, is the physical transport of the contaminant by the moving water

(Marino and Luthin, 1982). The second, molecular diffusion, is the movement of the contaminant due to concentration gradients. Migration is essentially controlled by the relative importance of convection and diffusion processes. The importance of convection depends on the extent of pore water flow, which is controlled by the hydraulic conductivity.

Hydraulic conductivity (k) is a measure of the ease of flow of a fluid through the sediment under a given hydraulic gradient (McLean and Grible, 1985); k is linked to permeability (a rock index property), and also to viscosity and density of the fluid. Darcy's law defines k: for one-dimensional flow, the velocity of the fluid moving through the sediment is proportional to the hydraulic gradient. The constant of proportionality is k, so that $v = ki$.

Sediments from the Peru margin are rich in organic matter and biogenous silica. They have unique physical properties, including very high undrained peak shear strengths, low remolded strengths, and high porosities and water contents to great depths (Hill and Marsters, this volume; Lee et al., this volume; Keller, 1983; Busch and Keller, 1981). These unique properties are attributed to organic bonding (Keller, 1983) dolomitization, and the incompressibility of the diatom skeletons (Hill and Marsters, this volume). We suspect that the resulting structure may also control the hydraulic conductivity characteristics.

The objective of this study is to examine the hydraulic conductivity (convective flow under pressure gradients) of sediment samples from the Peru margin obtained during Leg 112. Constant-head tests were performed on two samples, one from Site 679 and the other from Site 681, using a back-pressured odometer apparatus. Flow rates were measured after application of several increasing stress increments, corresponding to decreasing void ratios, for each sample. At each void ratio, several gradients were used to check that the flow data followed Darcy's law.

We suspected that conditions of high-gradient flow may cause changes in sediment fabric, such as alignment of diatoms in the direction of flow in association with a micropiping of clay particles from the interstitial spaces. Lindsley-Griffin et al. (this volume) found that dewatering veins often contain diatoms oriented in the direction of flow. Three types of samples (undisturbed, consolidated, and consolidated with hydraulic conductivity test performed) were examined using the scanning electron microscope (SEM) in an attempt to determine whether any changes in fabric occurred during testing.
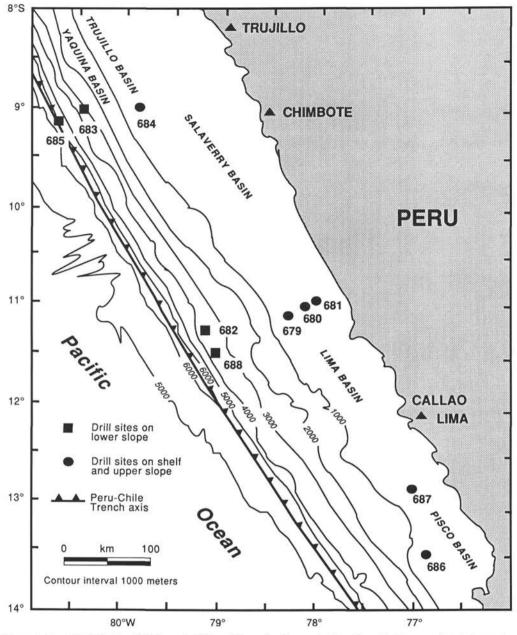
Figure 1. Leg 112 drill sites (679 through 687) and the major forearc basins along the Peru continental margin. The structural highs are shown as stippled areas. Bathymetry is in meters (modified from Suess, von Huene, et al., 1988).

METHODS

Whole-round samples, 10 cm long, were obtained for this study from good-quality hydraulic piston cores at Sites 679 and 681. The samples were capped and sealed in wax immediately and placed in cold storage. These sealed samples were placed in saltwater upon arrival at the test laboratory and maintained at 4°C until tested. Gas exsolution during core recovery precluded sampling for undisturbed physical properties for testing of the sediments at depths greater than 80 meters below seafloor (mbsf).

Each sample was prepared by inserting a stainless steel thin-walled ring with a cutting edge into the end of the 10-cm core. Once the ring was embedded in the sample, the sample and ring were extruded together from the plastic core liner. The sediment around the ring and at both ends was carefully trimmed. The sample was then transferred to the cell of a back-pressured consolidation system equipped for constant-head hydraulic conductivity testing. A back pressure of 300 kPa was applied to the sample for 72 hr to ensure complete saturation.

A description of the equipment and procedures followed is found in Silva et al. (1981).

Casagrande's (1936) construction was used to estimate the "pre-consolidation stress" (σ_c'), defined by Casagrande as the maximum past stress felt by the sample. This value is often compared to the effective overburden stress (σ_o') in the form of the ratio of σ_c'/σ_o', called the overconsolidation ratio (OCR). However, the usefulness of this parameter deteriorates near the seafloor as σ_o' approaches zero and OCR approaches infinity. Lee et al. (this volume) used the excess maximum past stress, σ_c' (equal to $\sigma_c' - \sigma_o'$) to examine consolidation data for sediment from the Peru margin, and the same calculation is used here to allow comparison. The samples were allowed to reach the end of primary consolidation (log-of-time method) under applied stress increments ranging from 512 to 4096 kPa. These stresses correspond, using rough calculations, to 140 to 1120 mbsf if normally consolidated conditions are assumed, or 70 to 560 mbsf if an estimated mean OCR of 2 is assumed.
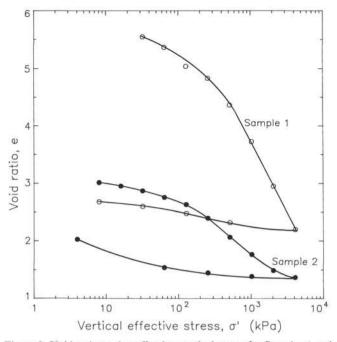
Figure 2. Void ratio vs. log effective vertical stress for Samples 1 and 2. Sample 1 exhibits the higher initial void ratio and higher compression index, reflecting the differences in the two samples.

Increasing stress increments helped establish Darcy's law over a range of consolidation states by reducing the void ratio of the sample. When the end of primary consolidation was reached for each stress increment, the loading platen of the consolidation cell was locked in place, ensuring no further consolidation or swelling during the hydraulic conductivity test. Constant-head tests then were performed at different hydraulic gradients for each stress level. Gradients in the range of 50 to 600 were selected to provide plots of flow velocity vs. hydraulic gradient. Gradients are calculated as the ratio of the head difference to the flow length. Flow for all tests was in the upward vertical direction. De-aired, filtered seawater (salinity of 35 ppt) was used as the permeant.

Subsamples were prepared for SEM analysis to examine changes in sediment fabric that may have occurred during consolidation and hydraulic conductivity testing. The disk-shaped consolidation samples were broken by hand so that a vertical plane surface was exposed. A thin (2–3 mm) sample was then cut, while ensuring that the broken surface was undisturbed. Three different sample types were obtained: undisturbed sediment, sediment consolidated to 1024 kPa, and sediment consolidated to 1024 kPa and then subjected to hydraulic gradients up to 200 during a constant-head test. The samples were air-dried, mounted on SEM stubs with epoxy, and gold-coated.

Atterberg limits results were classified using the method devised by Casagrande (1948). Grain-size tests were performed using the methods described in ASTM Standard D-2217-78 and D-422-63; 0.075 mm defines the sand/silt boundary and 0.005 mm the silt/clay boundary. Reported water contents are percentages based on the dry weight of the sample. Bulk density is the ratio of the mass of wet sample to the volume of wet sample. Volumes were measured using a penta-pycnometer. Void ratio was calculated as the ratio of the volume of voids to the volume of solids. Values obtained for index properties were corrected for saltwater content using formulas derived by Noorany (1984).

RESULTS AND DISCUSSION

Constant-head tests were performed on two samples. The first, Sample 112-679C-8H-2, 140–142 cm (68.9 mbsf) here is called Sample 1, and the other, Sample 112-681C-2H-3, 144–146 cm (10.3 mbsf) has been named Sample 2.

Differences between the two samples are indicated by index property data as well as by consolidation and perme-

ability test results. Grain size analysis of Sample 1 indicates it consists predominantly of silt (65%), with 9% sand and 26% clay. The analysis for Sample 2 indicates a sandy silt (61% silt, 35% sand) with trace clay (4%). The size distribution obtained for Sample 2 is coarser than most measured for these shelf sediments. However, core and smear slide descriptions indicate that zones of increased sand content occur (Hill and Marsters, this volume; Suess, von Huene, et al., 1988b). Sample 2 was obtained from the most landward core and could be expected to have more detrital influx.

Sample 1 was the deeper of the two samples, taken at 68.95 mbsf. However, this sample had a higher water content (199%) than Sample 2, which was taken from 10.36 mbsf and had a water content of 103%. The anomalous trend in water content can likely be attributed to higher biogenic content reflected by the higher clay and lower sand contents of these sediments.

Atterberg limit analyses performed on the two samples resulted in a liquid limit of 118% and plastic limit of 54% for Sample 1, and a liquid limit of 122% and plastic limit of 93% for Sample 2. The plasticity index (calculated as the difference between liquid limit and plastic limit) is higher for Sample 1 and again reflects the higher clay content of this sample, i.e., the sample with more clay is plastic over a larger range of water contents than the other sample. Hill and Marsters (this volume) divided samples into three facies categories—laminated biogenic, bioturbated, and terrigenous—on the basis of physical properties data. Sample 1 has properties comparable to the "laminated" facies, and Sample 2 behaves similarly to the "terrigenous" facies.

Using the Unified Soil Classification System (Casagrande, 1948), both samples can be classified as "MH—inorganic silts, micaceous or diatomaceous fine sandy or silty soils" or "OH—organic clays of medium to high plasticity, organic silts." Because grain size analyses have shown the samples to be predominantly silt, the "diatomaceous silty soils" classification is the appropriate one. These results are comparable to others from the Peru margin reported by Hill and Marsters (this volume), Lee et al. (this volume), and Keller (1983).

Interestingly, the natural water content (199%) exceeds the liquid limit (118%) for Sample 1. This phenomenon was also reported by Hill and Marsters (this volume), Lee et al. (this volume), and Keller (1983). Keller noted that, with natural water contents that exceed the liquid limits, the Peru margin sediment could collapse upon shear failure and undergo large strain flowlike deformation.

Void ratio vs. effective vertical stress for the consolidation data of Samples 1 and 2 are presented in Figure 2. Sample 1 had a much higher initial void ratio ($e = 5.6$) than Sample 2 ($e = 3.1$), and also exhibited a higher compression index (C_c, rate of change in void ratio with a tenfold increase in vertical effective stress at stress levels greater than the maximum past stress). These data again reflect the differences in the index properties values of the two samples.

Both samples exhibit apparent overconsolidation (i.e., $\sigma_c' > \sigma_o'$). Sample 1 has a calculated $\sigma_c' = 180$, $\sigma_o' = 34$, and $\sigma_e' = 146$. Sample 2 has a calculated $\sigma_c' = 380$, $\sigma_o' = 160$, and $\sigma_e' = 220$. These results correlate well with those obtained by Lee et al. (this volume) for samples from the same sites. Flow velocity vs. hydraulic gradient at different void ratios are shown for Samples 1 and 2 in Figures 3 and 4, respectively. Linear least squares fit of data from both tests indicate the presence of threshold gradients. Examination of the flow data indicates that the velocities measured during the tests were large enough so that equipment error was not a factor in this discrepancy.
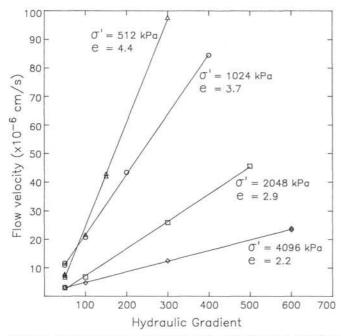
Figure 3. Flow velocity vs. hydraulic gradient for Sample 1. The four curves are for four different void ratios.
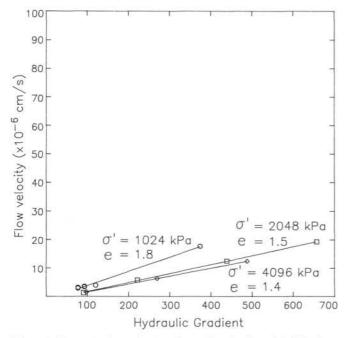

Figure 4. Flow velocity vs. hydraulic gradient for Sample 2. The three curves are for three different void ratios.

The data for many of the stress increments would be better represented by concave-upward curves. Darcy's law assumes a linear relationship between velocity of fluid moving through the sample and hydraulic gradient, with k, the coefficient of hydraulic conductivity, as the proportionality constant. However, nonlinear flow has been reported, and there has been considerable debate by scientists (Al-Tabbaa and Wood, 1987; Silva et al., 1981; Pane et al., 1983; Mitchell and Younger, 1967) regarding the applicability of high-gradient hydraulic conductivity test results for the analysis of field behavior.

Changes occurring in the sediment fabric during successive loading and inducement of high-gradient flow probably caused
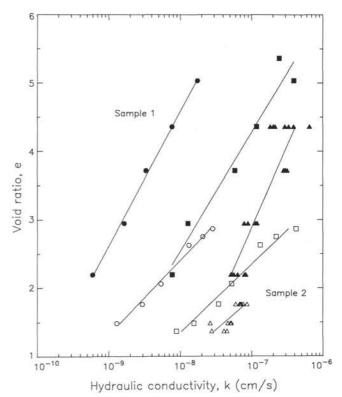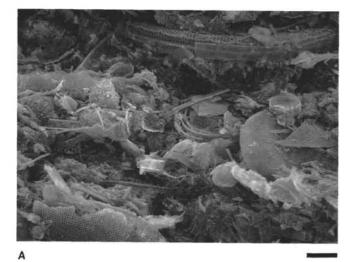

Figure 5. Void ratio vs. hydraulic conductivity for Samples 1 and 2. Sample 1 data are shown as solid symbols, while Sample 2 data are shown as open symbols. Three types of data are shown for each sample. The k was calculated from the log time (shown as circles) and root time (shown as squares) consolidation data as well as measured directly from the constant-head test (shown as triangles).
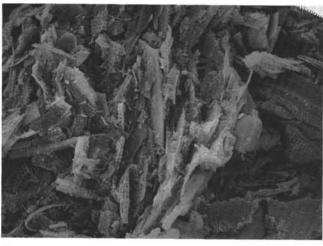
the observed behavior. If high-gradient flow caused formation of conduits and thus allowed increased flow rates during the measurement, the curves would take on a concave-upward trend. More testing, at lower gradients, will be needed to determine whether this threshold gradient is real or the result of sample disturbance during high-gradient testing.

In addition to the values obtained by direct measurement during the constant-head tests, the coefficient of hydraulic conductivity, k, was also calculated from the log-of-time and root-of-time consolidation data (Terzaghi and Peck, 1967). The calculated hydraulic conductivity obtained from these methods rarely agrees with each other or with values obtained from direct measurements (Sandbaekken et al., 1986; Bryant et al., 1981; Clukey and Silva, 1981). The equations used to calculate hydraulic conductivity from consolidation data (Terzaghi and Peck, 1967) do not account for secondary compression and thus underestimate the coefficient of hydraulic conductivity. Secondary compression effects are more significant in the log-of-time method.

Calculated and measured values of k vs. void ratio for Samples 1 and 2 are presented in Figure 5. Differences between the direct measurement values and those calculated from square-root-of-time and log-of-time consolidation data are comparable to those reported in the literature. Scattered k values were attributed to the difficulty in interpreting the time curves when primary consolidation occurs rapidly.

SEM analysis of an undisturbed sample (112-679C-7H-5, 140–142 cm; 63.90 mbsf) showed diatoms and clay in a random structure. Figure 6A is a photograph of an SEM image (1000× magnification) of a sample (112-679C-7H-5, 145–147 cm; 63.95 mbsf) that has been consolidated to 1024 kPa. Note the

A

B

Figure 6. A. Photograph of an SEM image (1000× magnification) of a sample (112-679C-7H-5, 145–147 cm) that has been consolidated to 1024 kPa. Note the presence of many diatom fragments, the result of consolidation under the vertical stress applied during the consolidation test. B. Photograph of an SEM image (1000× magnification) of a sample (112-679C-8H-2, 138–140 cm) that has been consolidated to 1024 kPa, followed by a permeability test. Most of the large diatoms show no movement due to flow through the sample, as seen at the edges of the photograph. However, there are areas in which vertical "conduits" appear to be packed with diatom fragments, as seen in the center of the photograph. Flow through the sample was in the vertical upward direction.

presence of many diatom fragments. Fragmenting was not observed in analyses of the undisturbed sample and is the result of the vertical stress applied during the consolidation test. However, the structure is still random.

Al-Tabbaa and Wood (1987) measured hydraulic conductivity in two directions and found that as a clay sample was consolidated one-dimensionally, anisotropy in the clay fabric resulted in horizontal coefficients of hydraulic conductivity much greater than vertical hydraulic conductivity at all void ratios. If horizontal conductivities are greater, then horizontal flow could control the rate of consolidation of the sediment *in situ*, taking into account the drainage path, and consolidation could occur faster than one-dimensional consolidation tests with vertical drainage would indicate. However, if the struc-

ture of a diatomaceous sediment remains fairly random despite increasing vertical stress, as is indicated by the results of testing of physical properties and SEM analyses, then horizontal and vertical permeabilities would be expected to remain comparable.

Figure 6B is a photograph of an SEM image (1000× magnification) of a sample (112-679C-8H-2, 138–140 cm; 68.88 mbsf) that has been consolidated to 1024 kPa, followed by induced upward flow. Most of the sample exhibits characteristics similar to the sample with no constant-head test performed. In general, there is no apparent reorientation of the larger diatoms as a result of the flow of water through the sample. However, as shown in Figure 6B, there were areas in the sample in which vertical "conduits" appear to be packed with diatom fragments. This is similar to characteristics found in fluid escape structures observed in these sediments (Lindsley-Griffin et al., this volume).

The data for Samples 1 and 2 indicate a sediment of low hydraulic conductivity, particularly at lower void ratios. The values obtained for k fall within a typical range (Terzaghi and Peck, 1948) for a silty clay. These results do not correspond to the measured grain-size data. We also expected that the porous fabric indicated in other physical-properties analyses would result in higher values of k. It is likely that diagenesis of the sediment has resulted in unconnected pore spaces. The lack of well-connected void spaces would make these sediments highly impermeable in their natural condition.

Micro- or macro-fractures may be important in the transmission of fluid in these highly impermeable sediments. If an impermeable layer in a consolidating sediment sequence exists, it may act as a trap for fluids percolating up through the sediments during consolidation. Brittle deformation may release excess pressures, resulting in micro-faults (Hill and Marsters, this volume) along which fluid movement might occur.

This study provides a preliminary estimate of k, hydraulic conductivity, caused by pore pressure gradients for the sediment of the Peru margin. Further testing will be performed to address a number of concerns from this work. Testing at lower gradients is needed to establish the shape of velocity-gradient curves at gradients more likely to occur *in situ*. Testing of samples from different depths at the same site will allow for a better understanding of the effects of diagenesis on hydraulic conductivity. In these sediments chemical potential gradients are also likely to influence migration of solutes and will be considered in future analyses in an attempt to estimate the relative importance of convection and diffusion in diagenetic redistribution in the Peru margin sediments.

CONCLUSIONS

Values of hydraulic conductivity in the range of 10^{-9} to 10^{-6} cm/s were measured during constant-head tests for samples with void ratios of 1.3 to 5.5. These hydraulic conductivity values fall within a typical range for silty clay, although grain-size analyses characterize the material as predominantly (approximately 65%) silt. Diagenesis may result in a reduction of the number of well-connected pore spaces, thus increasing the length of the flow path and making these sediments highly impermeable. Flow through the sediments is most likely to occur along faults that are formed during deformation of the sediments.

REFERENCES

Al-Tabbaa, A., and Wood, D. M., 1987. Some measurements of the permeability of Kaolin. *Geotechnique*, 3(4):499–503.

Berner, R. A., 1980. *Early Diagenesis: A Theoretical Approach*: Princeton (Princeton University Press).

Bryant, W. R., Bennett, R. H., and Katherman, C. E., 1981. Shear strength, consolidation, porosity, and permeability of oceanic sediments. *In* Emiliani, C. (Ed.), *The Sea, Vol. 7: The Oceanic Lithosphere*: New York (Wiley), 1555–1616.

Busch, W. H., and Keller, G. H., 1981. The physical properties of Peru-Chile continental margin sediments—the influence of coastal upwelling on sediment properties. *J. Sediment. Petrol.*, 51:705–719.

Casagrande, A., 1936. The determination of the pre-consolidation load and its practical significance. *Proc., First Int. Conf. on Soil Mechanics and Foundation Engineering*, 3:60–64.

—————, 1948. Classification and identification of soils. *Trans., Am. Soc. Civil Engrs.*, 113:901.

Clukey, E. C., and Silva, A. J., 1981. Permeability of deep-sea clays: northwestern Atlantic. *Mar. Geotechnol.*, 5(1):1-26.

Keller, G. H., 1983. Coastal upwelling, its influence on the geotechnical properties and stability characteristics of submarine deposits. *In* Suess, E., and Thiede, J. (Eds.), *Coastal Upwelling: Its Sediment Record, Vol. 1*: New York (Plenum Press), 181–199.

Marino, M. A., and Luthin, J. N., 1982. Seepage and Groundwater (Developments in Water Science; 13): New York (Elsevier).

McLean, A. C., and Grible, C. D., 1985. *Geology for Civil Engineers*: London (Allen and Unwin).

Mitchell, J. K., and Younger, J. S., 1967. Abnormalities in hydraulic flow through fine-grained soils. Permeability and capillarity of soils. ASTM STP, 417:106–139.

Noorany, I., 1984. Phase relations in marine soils. *ASCE J. Geotech. Eng.*, 110(4):539–543.

Pane, V., Croce, P., Znidarcic, D., Ko, H.-Y., Olsen, H. W., and Schiffman, R. L., 1983. Effects of consolidation on permeability measurements for soft clay. *Geotechnique*, Tech. Note 33(1):67–72.

Rumer, R. R., Jr., 1972. On the derivation of a convective-dispersion equation by spatial averaging. *In Fundamentals of Transport Phenomena in Porous Media, Inter. Assoc. for Hydraulic Res.*: Amsterdam (Elsevier).

Sandbaekken, G., Berre, T., and Lacasse, S., 1986. Oedometer testing at the Norwegian Geotechnical Institute. *In* Yong, R. N., and Townsend, F. C. (Eds.), *Consolidation of Soils: Testing and Evaluation*. ASTM STP, 892:329–353.

Silva, A. J., Hetherman, J. R., and Calnan, D. I., 1981. Low-gradient permeability testing of fine-grained marine sediments. *Permeability and Groundwater Contaminant Transport*. ASTM STP, 746:121–136.

Suess, E., von Huene, R., and Leg 112 Shipboard Scientists, 1988a. ODP Leg 112: The Peru continental Margin—II, History and Geochemistry of Depositional Environment. *Geology*, 16(10):939–943.

Suess, E., von Huene, R., et al., 1988b. *Proc. ODP, Init. Repts.*, 112: College Station, TX (Ocean Drilling Program).

Terzaghi, K. and Peck, R. B., 1967. *Soil Mechanics in Engineering Practice*: New York (Wiley).